Quantifying the statistical complexity of low-frequency fluctuations in semiconductor lasers with optical feedback

J. Tiana-Alsina,[1,*] M. C. Torrent,[1,†] O. A. Rosso,[2,3,‡] C. Masoller,[1,§] and J. Garcia-Ojalvo[1,‖]

[1]*Departament de Física i Enginyeria Nuclear, Universitat Politécnica de Catalunya, Campus de Terrassa, Edif. GAIA, Rambla de Sant Nebridi s/n, Terrassa E-08222 Barcelona, Spain*

[2]*Departamento de Física, Instituto de Ciências Exatas, Universidade Federal de Minas Gerais, Av. Antônio Carlos, 6627 Campus Pampulha, C.P. 702, 30123-970 Belo Horizonte, MG, Brazil*

[3]*Chaos & Biology Group, Instituto de Cálculo, Facultad de Ciencias Exactas y Naturales, Universidad de Buenos Aires, 1428 Ciudad Universitaria, Buenos Aires, Argentina*

(Received 26 April 2010; published 19 July 2010)

Low-frequency fluctuations (LFFs) represent a dynamical instability that occurs in semiconductor lasers when they are operated near the lasing threshold and subject to moderate optical feedback. LFFs consist of sudden power dropouts followed by gradual, stepwise recoveries. We analyze experimental time series of intensity dropouts and quantify the complexity of the underlying dynamics employing two tools from information theory, namely, Shannon's entropy and the Martín, Plastino, and Rosso statistical complexity measure. These measures are computed using a method based on ordinal patterns, by which the relative length and ordering of consecutive interdropout intervals (i.e., the time intervals between consecutive intensity dropouts) are analyzed, disregarding the precise timing of the dropouts and the absolute durations of the interdropout intervals. We show that this methodology is suitable for quantifying subtle characteristics of the LFFs, and in particular the transition to fully developed chaos that takes place when the laser's pump current is increased. Our method shows that the statistical complexity of the laser does not increase continuously with the pump current, but levels off before reaching the coherence collapse regime. This behavior coincides with that of the first- and second-order correlations of the interdropout intervals, suggesting that these correlations, and not the chaotic behavior, are what determine the level of complexity of the laser's dynamics. These results hold for two different dynamical regimes, namely, sustained LFFs and coexistence between LFFs and steady-state emission.

DOI: 10.1103/PhysRevA.82.013819 PACS number(s): 42.65.Sf, 42.55.Px, 05.45.−a, 42.60.Mi

I. INTRODUCTION

Optical feedback effects in semiconductor lasers have been extensively investigated over the past two decades. They are relevant not only for practical applications in which the laser is subjected to feedback from an external reflector, but are also very interesting from a nonlinear dynamics point of view, as optical feedback can induce a rich variety of dynamical regimes, including multistability, excitability, and high-dimensional chaos. Many studies of these dynamical regimes exist, but no systematic quantification of the level of statistical complexity exhibited by these systems, in particular in the regime of chaotic dynamics, exists so far.

A well-known feedback-induced instability is the regime of low-frequency fluctuations (LFFs), which occur for moderate feedback and near the lasing threshold. The LFFs consist in sudden power dropouts arising at irregular times, followed by gradual, stepwise recoveries. The power dropouts are known to be actually a slow modulation of fast picosecond pulses [1,2]. A characteristic feature of LFFs is that, as the laser bias current increases, the average time interval between consecutive dropouts decreases, and the dropouts become increasingly frequent and begin to merge [3]. Thus, there is a gradual transition through which the output power becomes increasingly irregular with increasing bias current. For large-enough bias current no dropouts are observed, but rather a completely irregular intensity time trace arises, a regime which has been termed fully developed coherence collapse.

Another characteristic of the LFF regime is that, in a wide region of parameters, it coexists with stable emission, with the relative duration of the stable emission state and the LFF state depending on the bias current, the feedback strength, and the phase-amplitude coupling factor (α factor) [3–6]. The coexistence of LFFs and stable emission has raised the issue of whether the LFFs are a transient dynamics which turns into a sustained one due to the presence of noise. Several studies have focused on characterizing deterministic chaotic features of the dropouts [7,8], as well as stochastic properties [9]. It has been shown [10–13] that the α factor strongly influences the operation regime of the laser. For small α, the LFFs are transient for all levels of optical feedback, after which the laser settles into a stable operation mode; for intermediate values of α, the regime of sustained LFFs alternates with "windows" of transient LFFs; for large α, the laser operates in sustained LFFs [10,11].

In spite of the vast amount of research done on the LFF instability, the *statistical complexity* of this dynamical regime has, to the best of our knowledge, not been investigated so far. Here we address this issue from the perspective of information theory, which allows us to quantify the complexity of the LFF regime as it approaches fully developed coherence collapse, for increasing intensity of the laser's pump current.

*jordi.tiana@upc.edu
†carme.torrent@upc.edu
‡oarosso@fibertel.com.ar
§cristina.masoller@upc.edu
‖jordi.g.ojalvo@upc.edu

Most systems in nature are neither completely ordered nor completely disordered, but something in between. Within the framework of information theory, the statistical complexity of a system is zero in the extreme situations of complete knowledge (or "perfect order") and total ignorance (or "complete randomness"). Both are simple situations, as one is fully predictable and the other has a simple statistical description. In order to capture the diversity and the rich spectrum of unpredictability occurring between these two extreme situations, many statistical complexity measures have been proposed in the literature [14–23]. These are useful tools for analyzing high-dimensional dynamics presenting underlying, hidden, or unobserved states that might organize the system's behavior. Statistical complexity measures are particularly useful when there is no prior knowledge of the hidden dynamics. They have been used, for instance, to characterize spatiotemporal patterns [24], distinguish noise from chaos [25], and identify a transition from a healthy to a diseased state in the brain [26].

The LFF power dropouts, being a slow modulation of fast high-dimensional pulses, are a potentially interesting dynamical regime to be analyzed with complexity tools. Here, following Refs. [22,25], we employ the Martín, Plastino, and Rosso (MPR) statistical complexity measure $C[P]$, defined as a functional of the probability distribution function P that characterizes the state of the system. $C[P]$ is the product of the "disequilibrium," $Q[P]$, which measures the distance to the equilibrium state, and the normalized Shannon entropy, $H[P]$. Defined in this way, $C[P]$ can be expected to display a maximum somewhere between $H = 0$ (complete order) and $H = 1$ (complete disorder).

A crucial step for obtaining meaningful results is to define a probability distribution P that fully characterizes the system, that is, that captures the organization of the hidden fast dynamics underlying the LFF dropouts. While one could just define P in terms of the distribution of either intensity fluctuations or interdropout intervals, this would result in neglecting time correlations that may exist between consecutive dropouts. An alternative methodology, originally proposed by Bandt and Pompe (BP) [21], is based on "ordinal patterns" and makes it possible to define a probability distribution function that takes into account the time ordering of the dropouts. Even though this method ignores the precise timing of the dropouts and the absolute duration of the interdropout intervals, it reveals, as we show in what follows, interesting features in the transition from LFFs to fully developed coherence collapse (such as enhanced complexity accompanied by a decrease of the entropy).

This article is organized as follows: Section II describes the experimental setup and presents the quantification of the transition from LFFs to coherence collapse, in terms of two indicators that are commonly used in the literature: the average interdropout interval and the normalized standard deviation of the interdropout intervals. Section III presents the results of the analysis of the experimental time series using the BP method. We show that during the transition to coherence collapse, there is a region of enhanced complexity, accompanied by a decrease of the normalized entropy. Section IV contains a discussion of the results and the conclusions.

II. EXPERIMENTS

We consider a laser diode subject to optical feedback from an external cavity. The laser used in the experiment is an Al-Ga-In-P Fabry-Perot semiconductor laser (GHO6510B2A) operating at a nominal wavelength $\lambda_n = 650$ nm. The temperature and pump current of the laser are controlled with an accuracy of $\pm 0.01^{\circ}$C and ± 0.01 mA. For a temperature $T = 18.30^{\circ}$C, the threshold current of the solitary laser is $I_{\mathrm{th}} = 29.39$ mA. The round-trip time in the external cavity is 2.5 ns. The laser intensity is detected by a high-speed fiber photodetector with a bandwidth of 2 GHz (DET01CFC), whose signal is amplified using a 2-GHz high-speed amplifier (Femto) and sent to a 1-GHz oscilloscope (Agilent DS06104A). Due to the relatively low bandwidth of the detection system, we are only able to measure the slow feedback-induced dynamics (i.e., the LFF power dropouts) and not the fast picosecond pulses.

Power dropouts for three different values of the pump current are shown in Fig. 1, whose panel (a) represents the output intensity corresponding to a dynamical behavior where there is coexistence between stable emission and LFFs. As described in [3], within the coexistence region, the duration of the LFF intervals increases with the pump current and the feedback strength. In Fig. 1(b) the injection current is high enough to be outside of the coexistence region, and the laser intensity displays sustained LFFs. Due to the increment of the injection current, the time between consecutive dropouts is shorter. Finally, in Fig. 1(c), the injection current is high and the laser operates close to coherence collapse, characterized by highly irregular oscillations of the light intensity.

Time series with more than 10^4 dropouts were recorded for various values of the pump current. For low pump currents the dropouts are infrequent and very long time series had to be recorded; thus, a small sampling rate was used in the digital acquisition system. For high pump currents the dropouts are more frequent, and shorter time series were recorded with a larger sampling rate. The sampling rates

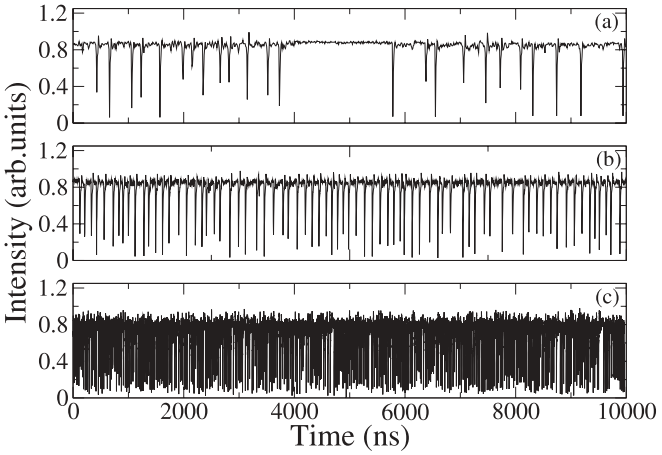

FIG. 1. Time traces for three different values of the pump current corresponding to three different dynamical regimes. (a) Coexistence of LFFs and stable emission, (b) sustained LFFs, and (c) transition to coherence collapse. $I_a = 31.20$ mA, $I_b = 32.40$ mA, and $I_c = 35.00$ mA. The horizontal scale is the same in the three panels.

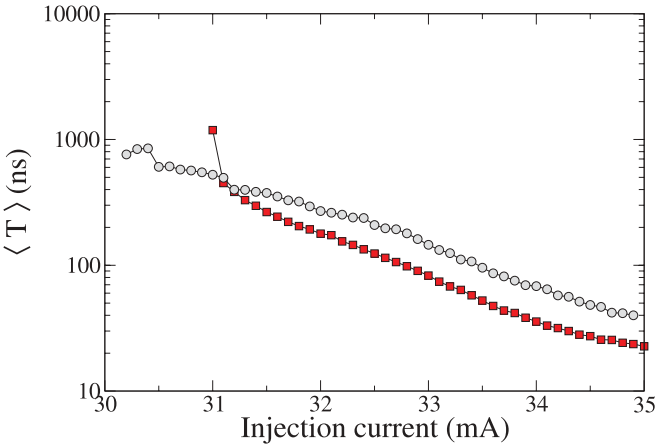

FIG. 2. (Color online) Mean value of the interdropout interval as a function of the pump current for two different experimental measurements that differ in the alignment of the external mirror and thus in the optical feedback strength. For one data set (referred to in the text as set I and indicated with circles) the mean interdropout interval is longer than for the other data set (set II, squares). This occurs in the entire range of variation of the injection current, except at the lowest current values in set II.

used in the experiments ranged from 250 megasamples/s to 1 gigasample/s.

III. STATISTICAL CHARACTERIZATION OF THE TIME SERIES

Figure 2 displays the mean time between consecutive dropouts, $\langle T \rangle$, as a function of the pump current, for two experimental realizations that differ in the alignment of the external mirror. This results in different couplings between the intracavity field and the reinjected field. The two couplings are distinct enough to lead to two different dynamical regimes [sustained LFFs (set I) and dynamic alternation of LFFs and stable emission (set II)], but similar enough to have a comparable threshold reduction due to the feedback (around 7%). As can be seen in Fig. 2, in the two sets of experimental measurements the mean time between consecutive dropouts decreases with the injection current, as mentioned previously. We have adjusted the experimental conditions such that the experimental conditions were as similar as possible, with the goal of analyzing data that were different only in their dynamical behavior.

In the next section we analyze via ordinal patterns the time-series measured under these different conditions and contrast their complexity measures. However, before computing the complexity of the time series, we first characterize them statistically. Figure 3(a) displays the normalized standard deviation of the interdropout interval (or coefficient of variation), $R = \sigma/\langle T \rangle$. Note that a decrease of R indicates enhanced regularity of the dropouts. Close to the solitary threshold (in the range from 30 to 32 mA) the increase of the injection current results in a decrease of R and the system becomes more regular. At an intermediate value of the pump current a minimum of R is reached, beyond which the dropouts become increasingly irregular, approaching coherence collapse, as the pump current increases further. As described in [7], the pump current affects

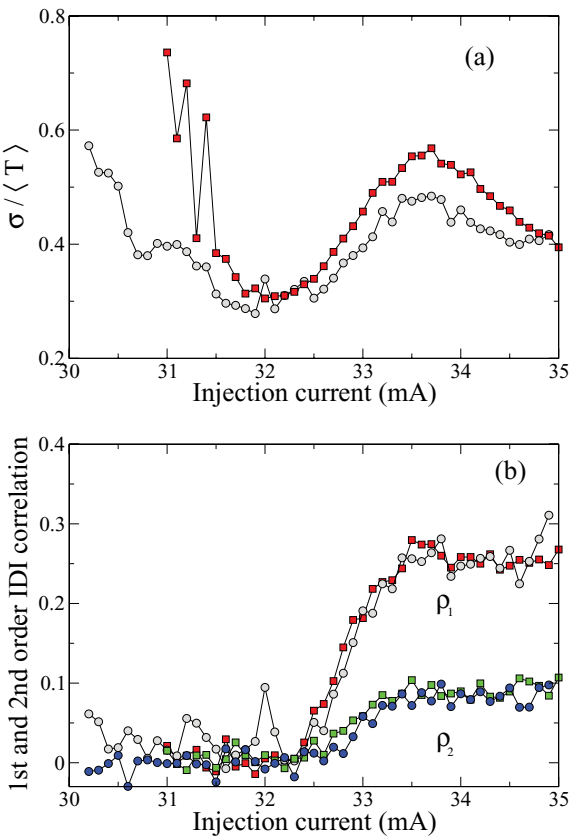

FIG. 3. (Color online) (a) Normalized standard deviation of the interdropout intervals (IDIs) as a function of the injection current, for two different experimental realizations. (b) First- and second-order IDI correlation coefficients as a function of the injection current, again for two different experimental realizations. Circles correspond to set I and squares to set II.

the fast dynamics, that is, the picosecond intensity pulses, differently than it affects the slow modulation, that is, the power dropouts. The fast pulses play the role of an effective noise, and thus the variation of the injection current results in a variation of the amplitude of the effective noise. Within that context, the existence of a minimum in the coefficient of variation for an intermediate pump current can be likened with the enhanced regularity of dropouts that arises for an optimal noise level in coherence resonance [27–29].

In Fig. 3(a) it can also be noticed that for one set of experimental measures R presents large fluctuations at low current values, while for the other set these oscillations are absent. As explained previously, the two sets of observations differ on the alignment of external mirror, and thus in the feedback strength. The large variations of R in data set II are due to the occurrence of a regime of coexistence of LFFs and stable emission, which is absent in the other data set. This behavior induces an error on R. Another statistical property of the data is the correlation of time intervals between consecutive dropouts (interdropout intervals, IDIs). The nth-order correlation coefficient between IDIs is defined as

$$\rho_n = \frac{\langle I_{k+n} I_k \rangle - \langle I_{k+n} \rangle \langle I_k \rangle}{\langle I_k^2 \rangle - \langle I_k \rangle^2}, \tag{1}$$

where $\{I_k\}$ is an ordered sequence of IDIs. Figure 3(b) shows the dependence of the first- and second-order IDI correlation coefficients on the pump current. A transition from a Markov to a non-Markov process is observed at a value of the pump around 32.5 mA, above which the correlations become nonzero (the second-order correlation being smaller than the first-order one). In what follows we will evaluate and compare the statistical complexity of both data sets.

IV. QUANTIFYING THE STATISTICAL COMPLEXITY

We begin by transforming the sequence of consecutive interdropout intervals $\{T_i, i = 1 \ldots M\}$ into a set of D-dimensional "ordinal patterns," following the BP method [21]. This is done by dividing the sequence $\{T_i\}$ into $M - D$ overlapping vectors of dimension D. Then, the value of T_i in a given vector is replaced with a number from 0 to $D - 1$, in accordance with the relative length of T_i in the ordered sequence (0 corresponding to the shortest T_i and $D - 1$ to the longest T_i in each vector). A third step is to compute the probability distribution P of the different vectors. Since the number of different vectors of dimension D is equal to $D!$, to have a good statistics one must have a large enough number of vectors, such that $M - D \gg D!$.

The last step is to compute the normalized Shannon entropy, $H[P]$, and the MPR statistical complexity, $C[P]$. The entropy is given by

$$H[P] = S[P]/S_{\max}, \tag{2}$$

where $S[P] = -\sum_{i=1}^{N} p_i \log p_i$ and $S_{\max} = \log N$, with $N = D!$ being the total number of vectors over which P is computed.

The MPR measure is defined as

$$C[P] = H[P] \cdot Q[P], \tag{3}$$

where $Q[P] = Q_0 J_S[P, P_e]$ quantifies the disequilibrium, calculated from the symmetric form $J_S[P_1, P_2]$ of the Kullback-Leiber relative entropy [30], $K[P_1|P_2]$ (i.e., $J_S[P_1, P_2] = (K[P_1|P_2] + K[P_2|P_1])/2$). P_e is the equilibrium distribution ($p_{i,e} = 1/N \; \forall \, i$) and Q_0 is a normalization constant,

$$Q_0 = -2\left\{\left(\frac{N+1}{N}\right)\ln(N+1) - 2\ln(2N) + \ln N\right\}^{-1}. \tag{4}$$

Figure 4 displays H and C for the the experimental data set where the feedback level is such that no coexistence is observed at low pump currents (set I); Fig. 5 displays H and C for the other data set (set II), for which there is coexistence between LFFs and stable emission at low pump currents. Results are presented for various values of the length of the ordinal patterns, D (embedding dimension). Since the experimental data series have about $M = 15\,000$ dropouts (set I) and $M = 10\,000$ dropouts (set II), in order to have a good statistics we limit ourselves to $D \leqslant 5$. We also display the results of analyzing the corresponding surrogate data, which consistently shows $H \sim 1$ and $C \sim 0$.

It can be observed that in both data sets, a region of enhanced statistical complexity, accompanied by a decrease of the normalized entropy, occurs at high-enough pump currents,

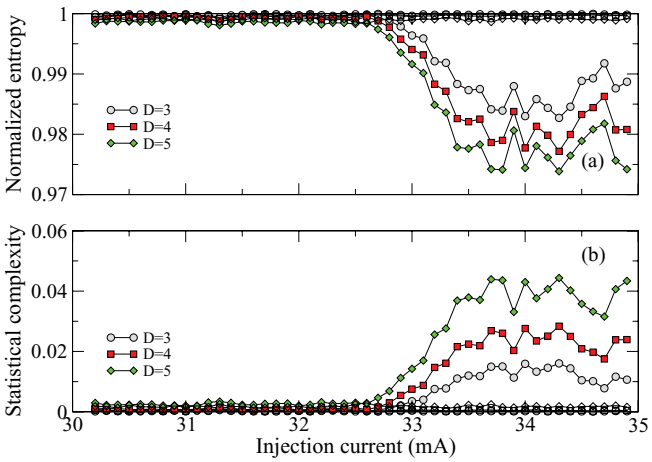

FIG. 4. (Color online) (a) Normalized Shannon entropy and (b) statistical complexity measure vs the laser injection current, for various values of the length of the ordinal patterns, D (embedding dimension). $M = 15\,000$. The data set is "set I," for which there is no coexistence of LFFs and stable emission at low injection currents. Open symbols represent the surrogate data for the filled symbols with the corresponding shape.

that is, around the transition between "regular" LFFs (where R is minimum; see Fig. 3) and highly irregular LFFs (approaching coherence collapse). The increase in the value of the complexity reveals that the distribution of ordinal vectors has a certain structure, in spite of the fact that the dynamics is highly stochastic. (Note that the normalized entropy is close to 1; however, it decreases in the region of increased complexity.) For low injection currents, the coexistence of LFF and stable emission is not detected, as $C \approx 0$ and $H \approx 1$ for both data sets. However, we remark that for the second data set, large oscillations of the normalized standard deviation are seen for low current in Fig. 3. This reveals a drawback of the BP

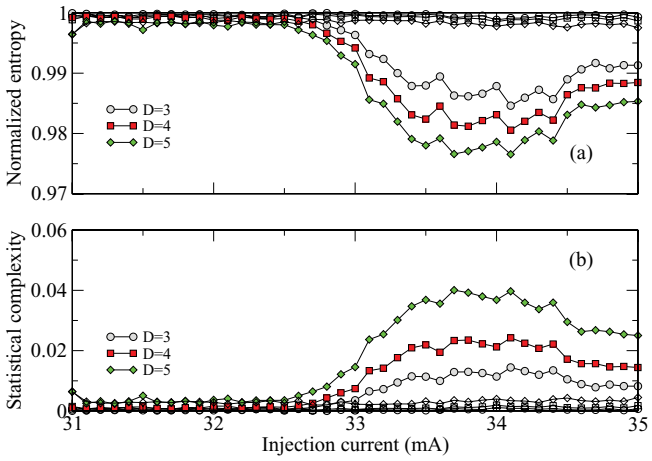

FIG. 5. (Color online) (a) Normalized Shannon entropy and (b) statistical complexity measure vs the laser injection current, for various values of the length of the ordinal patterns, D (embedding dimension). The data set is "set II," for which there is coexistence of LFFs and stable emission at low injection currents. $M = 10\,000$. Open symbols represent the surrogate data for the filled symbols with the corresponding shape.

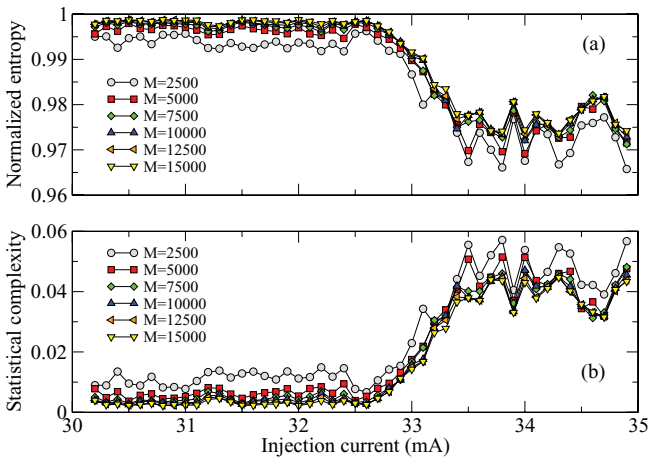

FIG. 6. (Color online) (a) Normalized Shannon entropy and (b) statistical complexity measure vs the laser injection current, for various values of the length of the time series, with $D = 5$. Note that C and H converge with increasing M. The data set used in this figure is set I.

methodology, which is due to the fact that the absolute length of the interdropout intervals is not considered, but only the relative order is taken into account.

It can be noticed that the analysis with the entropy and complexity measures agrees very well with that of the first- and second-order correlations in clearly displaying two qualitatively different regimes: one memoryless, occurring at low injection currents, and the other occurring at higher current values, for which there are memory effects revealed by time correlations. The second-order correlation coefficient is smaller than the first-order one, while an opposite effect is seen with the complexity measure C, which grows continuously as the ordinal pattern dimension D increases. This lack of convergence with respect to D can be interpreted as due to the finite size of the time series. To check this hypothesis, we display in Fig. 6 results of the analysis for fixed D and various values of the length of the time series. The figure shows that both C and H converge with increasing M. In other words, we speculate that if we could record experimentally a long-enough time series, such that we could use larger D values with good statistics, convergence would be seen with increasing D; that is, there would be an optimal D revealing the *finite* length of the memory of the system.

While we present here results only for two data sets, we have done extensive analysis of various experimental realizations and found that the results are robust, in the sense that characterizing the system in terms of the distribution of ordinal patterns captures enhanced complexity during the transition to coherence collapse; however, the enhanced regularity (i.e., the minimum of the indicator R) and the regime of LFF-stable emission coexistence are not detected.

V. DISCUSSION AND CONCLUSIONS

We interpret the results in the following terms: At low injection currents the dropouts are infrequent, there are long time intervals between consecutive dropouts, and therefore, the dropouts are statistically independent one of another: There are no memory effects and no patterns or correlations arise in the sequence of consecutive dropouts. For larger injection currents the dropouts are more frequent and there is some memory in the system; that is, there are time correlations revealed by $C \neq 0$ and $H \neq 1$. We believe that these correlations might arise because of the finite recovery time: The time when the next dropout occurs will depend on whether the laser fully recovered from the previous dropout. To conclude, we have shown that the normalized Shannon entropy and the MPR statistical complexity measure are suitable tools for quantifying subtle characteristics of the LFF dropouts and, in particular, the transition to fully developed coherence collapse as the laser bias current increases. However, the coexistence of LFF and stable emission at low bias currents, and the phenomenon of coherence resonance, for which the normalized deviation of the interdropout intervals displays a minimum at a certain bias current [27–29], are not detected.

ACKNOWLEDGMENTS

This research was supported in part by the Spanish Ministerio de Ciencia e Innovación through Project No. FIS2009-13360-C03-02, the Air Force Office Scientific Research through Project No. FA-8655-10-1-3075 (C.M.), the I3 program (J.G.O.), and the Agència de Gestió d'Ajuts Universitaris i de Recerca (AGAUR), Generalitat de Catalunya, through Project No. 2009 SGR 1168. C.M. and J.G.O. also acknowledge the ICREA Foundation for financial support. O.A.R. acknowledges partial support from CONICET, Argentina, and CAPES, Brazil.

[1] I. Fischer, G. H. M. van Tartwijk, A. M. Levine, W. Elsäßer, E. Göbel, and D. Lenstra, Phys. Rev. Lett. **76**, 220 (1996).
[2] G. Vaschenko, M. Giudici, J. J. Rocca, C. S. Menoni, J. R. Tredicce, and S. Balle, Phys. Rev. Lett. **81**, 5536 (1998).
[3] T. Heil, I. Fischer, and W. Elsäßer, Phys. Rev. A **58**, R2672 (1998).
[4] T. Heil, I. Fischer, and W. Elsäßer, Phys. Rev. A **60**, 634 (1999).
[5] T. Heil, I. Fischer, and W. Elsäßer, J. Opt. B **2**, 413 (2000).
[6] Y. Hong and K. A. Shore, IEEE J. Quantum Electron. **41**, 1054 (2005).
[7] J. F. Martinez-Avila, H. L. D. de S. Cavalcante, and J. R. Rios Leite, Phys. Rev. Lett. **93**, 144101 (2004).
[8] W. Ray, W-S. Lam, P. N. Guzdar, and R. Roy, Phys. Rev. E **73**, 026219 (2006).
[9] A. Hohl, H. J. C. van der Linden, and R. Roy, Opt. Lett. **20**, 2396 (1995).
[10] R. L. Davidchack, Y-C. Lai, A. Gavrielides, and V. Kovanis, Phys. Lett. A **267**, 350 (2000).
[11] R. L. Davidchack, Y-C. Lai, A. Gavrielides, and V. Kovanis, Physica D **145**, 130 (2000).

[12] A. Torcini, S. Barland, G. Giacomelli, and F. Marin, Phys. Rev. A **74**, 063801 (2006).
[13] J. Zamora-Munt, C. Masoller, and J. Garcia-Ojalvo, Phys. Rev. A **81**, 033820 (2010).
[14] A. Lempel and J. Ziv, IEEE Trans. Inf. Theory **22**, 75 (1976).
[15] P. Grassberger, Int. J. Theor. Phys. **25**, 907 (1986).
[16] J. P. Crutchfield and K. Young, Phys. Rev. Lett. **63**, 105 (1989).
[17] R. Wackerbauer *et al.*, Chaos Solitons Fractals **4**, 133 (1994).
[18] S. Pincus, Chaos **5**, 110 (1995).
[19] R. Lopez-Ruiz, H. L. Mancini, and X. Calbet, Phys. Lett. A **209**, 321 (1995).
[20] M. Palus, Physica D **93**, 64 (1996).
[21] C. Bandt and B. Pompe, Phys. Rev. Lett. **88**, 174102 (2002).
[22] M. T. Martín, A. Plastino, and O. A. Rosso, Physica A **369**, 439 (2006).
[23] D. G. Ke and Q. Y. Tong, Phys. Rev. E **77**, 066215 (2008).
[24] F. Kaspar and H. G. Schuster, Phys. Rev. A **36**, 842 (1987).
[25] O. A. Rosso, H. A. Larrondo, M. T. Martin, A. Plastino, and M. A. Fuentes, Phys. Rev. Lett. **99**, 154102 (2007).
[26] K. Young, Y. Chen, J. Kornak, G. B. Matson, and N. Schuff, Phys. Rev. Lett. **94**, 098701 (2005).
[27] G. Giacomelli, M. Giudici, S. Balle, and J. R. Tredicce, Phys. Rev. Lett. **84**, 3298 (2000).
[28] J. M. Buldú, J. Garcia-Ojalvo, C. R. Mirasso, M. C. Torrent, and J. M. Sancho, Phys. Rev. E **64**, 051109 (2001).
[29] J. M. Buldú, J. Garcia-Ojalvo, and M. C. Torrent, Phys. Rev. E **69**, 046207 (2004).
[30] S. Kullback and R. A. Leibler, Ann. Math. Stats. **22**, 79 (1951).